Shoreline Extraction Using Water Indices for Nautical Chart Assessment: A Case Study of Hua Hin Beach, Thailand

อารีย์ หวันหละเบ๊ะ[1*] และ ภัทราพร สร้อยทอง[2]
Aree Hwanlabeh[1*] and Phattraporn Soytong[2]

Received: June 2, 2025
Revised: June 4, 2025
Accepted: June 10, 2025

Abstract

Shoreline change is a crucial indicator of coastal dynamics, impacting maritime navigation, coastal planning, and nautical chart accuracy. In Thailand, traditional hydrographic surveys are limited by time and resources, resulting in outdated shoreline data. This study investigates the use of satellite-based remote sensing and geospatial analysis to assess shoreline change along Hua Hin Beach from 2012 to 2024.

Multi-temporal Landsat imagery from five periods, spaced three years apart, was analyzed using six spectral water indices: NDWI, MNDWI, AWEIsh, AWEInsh, LSWI, and WI2015. The analysis was conducted using Google Earth Engine in combination with the geemap Python API on Google Colab. Shoreline positions extracted with each index were compared to a reference shoreline from Thai nautical chart No.246 (edition 2012), using 430 validation points at 90-meter intervals. Accuracy was evaluated using RMSE and MAE, with WI2015 showing the highest accuracy (RMSE = 7.156 meters).

The best results from WI2015 were used in the Digital Shoreline Analysis System (DSAS) to compute shoreline change metrics; EPR, SCE, and NSM, across 380 transects. The results showed

[1*]ประจำกรมอุทกศาสตร์ กองทัพเรือ
Attached to Hydrographic Department, Royal Thai Navy
Email: nui.hydro@gmail.com
[2]ผู้ช่วยศาสตราจารย์ ภาควิชาภูมิสารสนเทศ คณะมนุษยศาสตร์และสังคมศาสตร์ มหาวิทยาลัยบูรพา
Assistant Professor, Department of Geoinformatics, Faculty of Humanities and Social Science, Burapha University
Email: phattraporn@go.buu.ac.th
*Corresponding Author

accretion in Zones A and E, erosion in Zones B and C, and stability in Zone D. Based on NSM, shoreline change was classified into Stable (<10 m), Moderate (10–50 m), and Significant (>50 m) categories for resurvey prioritization.

This study highlights the effectiveness of integrating satellite-derived water indices with DSAS for monitoring shoreline change and updating nautical charts in coastal zones.

Keywords: Shoreline Extraction, Water Index, Google Earth Engine, DSAS, Nautical Chart

1. Introduction

Coastal zones are dynamic interfaces between land and sea that are vital for ecological balance, economic activities, and human settlements. Shoreline change, manifested through erosion and accretion, is a critical indicator of coastal dynamics and has profound implications for maritime safety, land use planning, ecosystem stability, and the accuracy of nautical charts [1, 2]. In recent decades, both natural forces such as sea level rise, tides, and storms, as well as anthropogenic factors like coastal development and infrastructure expansion, have accelerated shoreline transformation [3, 4].

Traditional shoreline surveys conducted through hydrographic methods are often costly, time-consuming, and spatially limited. Consequently, shoreline data in many regions, including Thailand, are often outdated or incomplete, posing risks for navigation and resource management. The International Hydrographic Organization (IHO) emphasizes the need for regularly updated coastal data to maintain safe and efficient maritime operations [5]. According to the IHO S-44 standards, the positional uncertainty of the coastline depicted on nautical charts should not exceed 10 meters, particularly in areas critical to navigation.

Remote sensing and Geographic Information System (GIS) technologies offer an effective alternative to conventional field-based approaches. With the availability of multi-temporal satellite data and powerful cloud-based geospatial platforms such as Google Earth Engine [6], it is now feasible to conduct long-term shoreline monitoring with high spatial and temporal consistency. Spectral water indices applied to satellite imagery have proven particularly useful in delineating land–water boundaries, enabling the automated or semi-automated extraction of shoreline positions [7, 8].

This study aims to utilize Landsat satellite imagery and spectral indices to analyze shoreline changes along Hua Hin Beach, a coastal city in Prachuap Khiri Khan Province, Thailand. The region is both a tourist destination and an area of active coastal transformation due to natural processes and human pressures. Accurate detection of shoreline movement in this area is crucial for updating nautical charts, identifying erosion-prone zones, and informing sustainable coastal planning strategies. By integrating satellite image processing, spectral index classification, and shoreline change modeling using the Digital Shoreline Analysis System (DSAS), this study seeks to offer a robust, replicable framework for shoreline monitoring in tropical coastal environments.

The findings contribute not only to improved charting accuracy but also to coastal vulnerability assessment and long-term environmental management. Ultimately, this work aligns with global efforts to leverage Earth observation technologies for sustainable coastal development and maritime safety.

2. Objectives

The dynamic nature of coastal environments, especially in areas with growing human activities and natural pressures, necessitates effective monitoring and analysis of shoreline change. This study focuses on applying remote sensing and geospatial techniques to support shoreline extraction and nautical chart assessment in the Hua Hin coastal zone. The specific objectives are outlined as follows:

2.1 To investigate the methods used for shoreline extraction from satellite imagery along the beach of Hua Hin district, Prachuap Khiri Khan Province, Thailand during the period from 2012 to 2024

2.2 To evaluate the performance of various water indices when applied to satellite images for shoreline extraction and determine the most accurate index.

2.3 To analyze the patterns and trends of shoreline changes based on the shoreline extraction data and assess whether any areas along the Hua Hin beach require new nautical chart surveys.

3. Literature Reviews

Numerous studies have demonstrated the application of spectral indices for shoreline detection. McFeeters [8] introduced the Normalized Difference Water Index (NDWI) to enhance water–land contrast, while Xu [9] proposed the Modified NDWI (MNDWI) using SWIR for improved water detection in urban areas. Feyisa et al. [10] developed the Automated Water Extraction Index (AWEI), with variants for shadowed and non-shadowed conditions.

Fisher et al. [11] introduced Water Index 2015 (WI2015), incorporating multiple spectral bands, which has shown improved performance in heterogeneous landscapes. Bishop-Taylor et al. [12] emphasized the need for sub-pixel accuracy and band sensitivity analysis in shoreline detection.

For shoreline change analysis, the U.S. Geological Survey's DSAS has been widely adopted [13], allowing computation of metrics such as End Point Rate (EPR), Shoreline Change

Envelope (SCE), and Net Shoreline Movement (NSM). Song et al. [14] applied DSAS for long-term coastal monitoring in East Asia, while Isha and Adib [15] demonstrated their integration in GIS-based shoreline studies in Southeast Asia.

Google Earth Engine [6] has further enabled large-scale satellite data processing. Combined with validation datasets such as nautical charts [5, 16], this creates a reliable foundation for hydrographic decision-making.

4. The Methods of Research

This study investigates shoreline changes along Hua Hin Beach, Thailand, using a remote sensing and geospatial analysis framework. The process includes satellite data acquisition, spectral water index computation, shoreline extraction, accuracy validation, and shoreline change analysis using the Digital Shoreline Analysis System (DSAS). The overall technical workflow is illustrated in Figure 1.

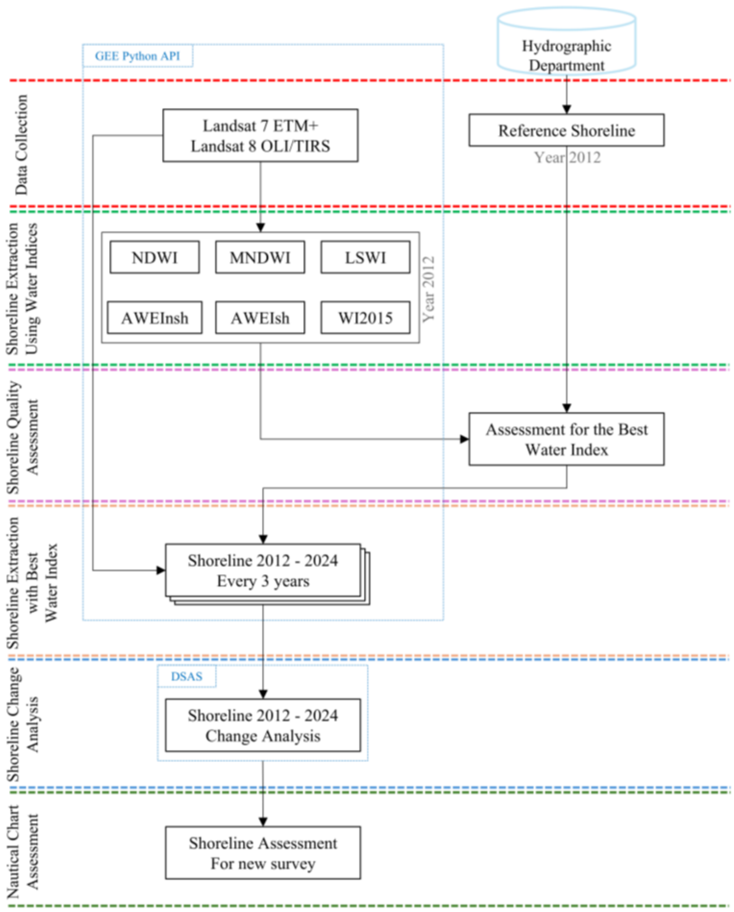

Figure 1 Technical Workflow of the Study

Landsat imagery was selected for five temporal intervals: 2012, 2015, 2018, 2021, and 2024. Images were sourced from Landsat 7 ETM+ for the first two periods and Landsat 8 OLI/TIRS for the latter three. The selection was based on low cloud cover, favorable tidal conditions, and minimal atmospheric interference. Preprocessing steps included top-of-atmosphere reflectance conversion and cloud masking using the pixel quality assurance (QA) bands in Google Earth Engine (GEE). Landsat 7 data were corrected for scan line errors using a linear interpolation method following the approach of Storey et al. [17]. All processing was conducted using GEE within a Python environment through Google Colab and the geemap API.

Six spectral water indices were employed to enhance the detection of water–land boundaries from satellite imagery. Each index offers distinct advantages depending on surface conditions, land cover, and image characteristics.

The Normalized Difference Water Index (NDWI), proposed by McFeeters [8] , enhances open water features by increasing the contrast between water and land. It utilizes the strong reflectance of water in the green band and absorption in the near-infrared (NIR) band, is calculated as:

$$NDWI = \frac{Green-NIR}{Green+NIR} \tag{1}$$

NDWI is effective in detecting surface water in natural environments but may perform poorly in built-up areas due to spectral confusion with impervious surfaces.

To address this limitation, the Modified NDWI (MNDWI), introduced by Xu [9] , replaces the NIR band with the shortwave infrared band (SWIR1), which helps to suppress noise from built-up features and enhances the separability of water bodies in urbanized or mixed land cover regions as:

$$MNDWI = \frac{Green-SWIR1}{Green+SWIR1} \tag{2}$$

The Automated Water Extraction Index for Shadow (AWEIsh) is specifically designed to minimize the confusion between water and shadowed areas, especially in mountainous or forested terrain. It accounts for multiple bands to distinguish water under complex illumination conditions and is calculated using:

$$AWEIsh = Blue + 2.5 * Green - 1.5 * (NIR + SWIR1) - 0.25 * SWIR2 \tag{3}$$

In contrast, the Automated Water Extraction Index for Non-Shadow (AWEInsh) is tailored for flat or well-illuminated regions without significant topographic shading. It emphasizes the contrast between water and non-water features while reducing false positives:

$$AWEInsh = 4 * (Green - SWIR1) - (0.25 * NIR + 2.75 * SWIR2) \quad (4)$$

The Land Surface Water Index (LSWI), commonly applied in agricultural and vegetated zones, is sensitive to soil moisture and water content in vegetation. It is especially useful for detecting water in floodplains, wetlands, or areas with partial vegetation cover, and is defined as:

$$LSWI = \frac{NIR - SWIR1}{NIR + SWIR1} \quad (5)$$

Finally, the Water Index 2015 (WI2015), proposed by Fisher et al. [11], integrates multiple spectral bands and empirically derived coefficients to optimize shoreline delineation. It is particularly effective in complex coastal environments due to its multi-band formulation and enhanced sensitivity to water features:

$$WI2015 = 1.7204 + (171 * Green) + (3 * Red) - (70 * NIR) - (45 * SWIR1) - (71 * SWIR2) \quad (6)$$

These indices were used to produce binary water–land masks from which shoreline positions were extracted using edge-detection methods. A summary of index equations and spectral band usage is presented in Table 1.

Table 1 Equations and References of Spectral Water Indices

Water Index	Equation	References
NDWI	$\frac{Green - NIR}{Green + NIR}$	[8]
MNDWI	$\frac{Green - SWIR1}{Green + SWIR1}$	[9]
AWEInsh	$4 * (Green - SWIR1) - (0.25 * NIR + 2.75 * SWIR2)$	[10]
AWEIsh	$Blue + (2.5 * Green) - \left(1.5 * (NIR + SWIR1)\right) - (0.25 * SWIR2)$	[10]
LSWI	$\frac{NIR - SWIR1}{NIR + SWIR1}$	[18]
WI2015	1.7204+(171*Green)+(3*Red)-(70*NIR)-(45*SWIR1)-(71*SWIR2)	[11]

The accuracy of each extracted shoreline was assessed using a reference shoreline digitized from the Thai nautical chart NC246 (edition 2012). A total of 430 control points were distributed at 90-meter intervals along the reference line. The distance from each index-derived shoreline to the corresponding reference point was computed using the Euclidean distance formula:

$$d_i = \sqrt{(x_2 - x_1)^2 + (y_2 - y_1)^2} \tag{7}$$

Where d_i represents the Euclidean distance between the estimated and reference shoreline points and (x_1, y_1), (x_2, y_2) are the coordinates of the extracted and reference shoreline points. Accuracy metrics included the Root Mean Square Error (RMSE) and the Mean Absolute Error (MAE), defined as:

$$RMSE = \sqrt{\frac{1}{N}\sum_{i=1}^{N} d_i^2} \tag{8}$$

$$MAE = \frac{1}{N}\sum_{i=1}^{N} d_i \tag{9}$$

These metrics quantify the positional error between the extracted and reference shorelines. The comparative results for all six indices are presented, and the one demonstrating the highest accuracy is selected for subsequent shoreline change analysis.

The index with the lowest RMSE, was selected for shoreline change analysis. Shoreline positions for each of the five years were used to detect temporal changes using DSAS version 5.0 in ArcGIS. A baseline was generated along the 2012 shoreline, and 380 transects were cast perpendicularly at 100-meter intervals.

DSAS computed several key metrics. The Net Shoreline Movement (NSM) measures the linear distance between the oldest and most recent shoreline. The End Point Rate (EPR) divides NSM by the number of years to determine the average annual change rate. The Shoreline Change Envelope (SCE) calculates the maximum variation between any two shorelines at each transect location. Additionally, Weighted Linear Regression (WLR) was applied to detect long-term trends in shoreline movement by fitting a regression line weighted by positional uncertainty over time, following the method described in Song et al. (2023).

To facilitate spatial interpretation, the study area was divided into five zones labeled A through E, progressing from north to south along the coast. The transects and zonal layout used for analysis are shown in Figure 2.

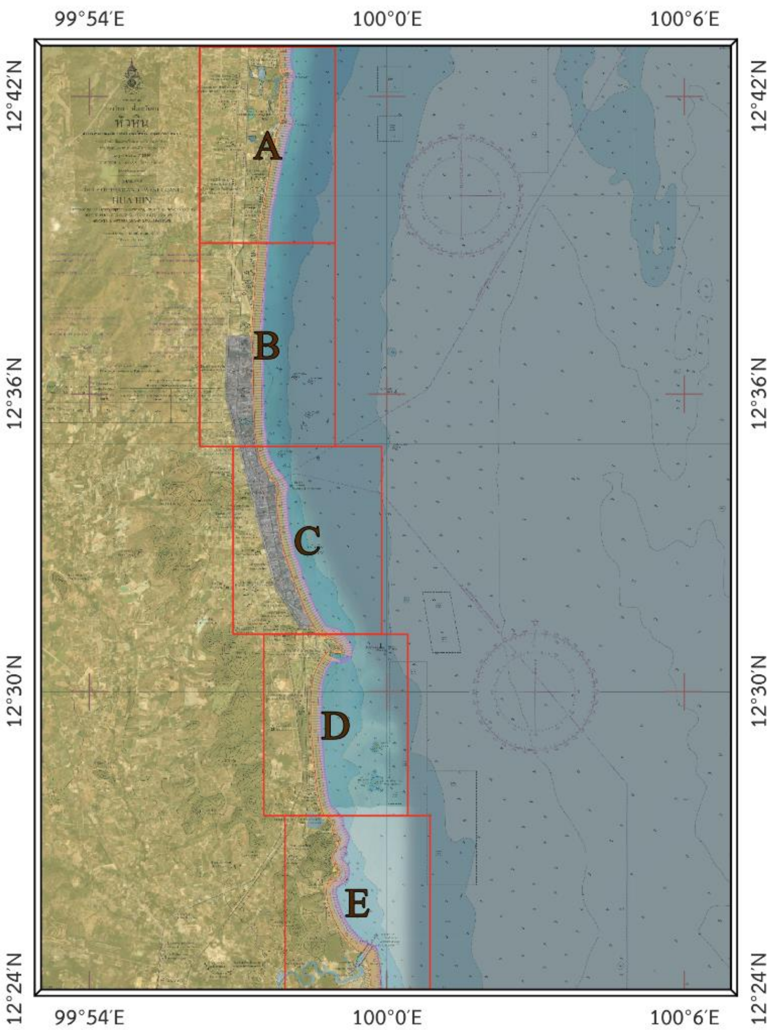

Figure 2 Transect and Zonal Map of Hua Hin Beach [19]

5. Results

The results of this study begin with a visual assessment of the water–land classification capability of each spectral water index. By applying threshold-based methods to Landsat imagery, initial classifications of water and non-water areas were produced to evaluate how effectively each index distinguishes shoreline boundaries prior to quantitative validation.

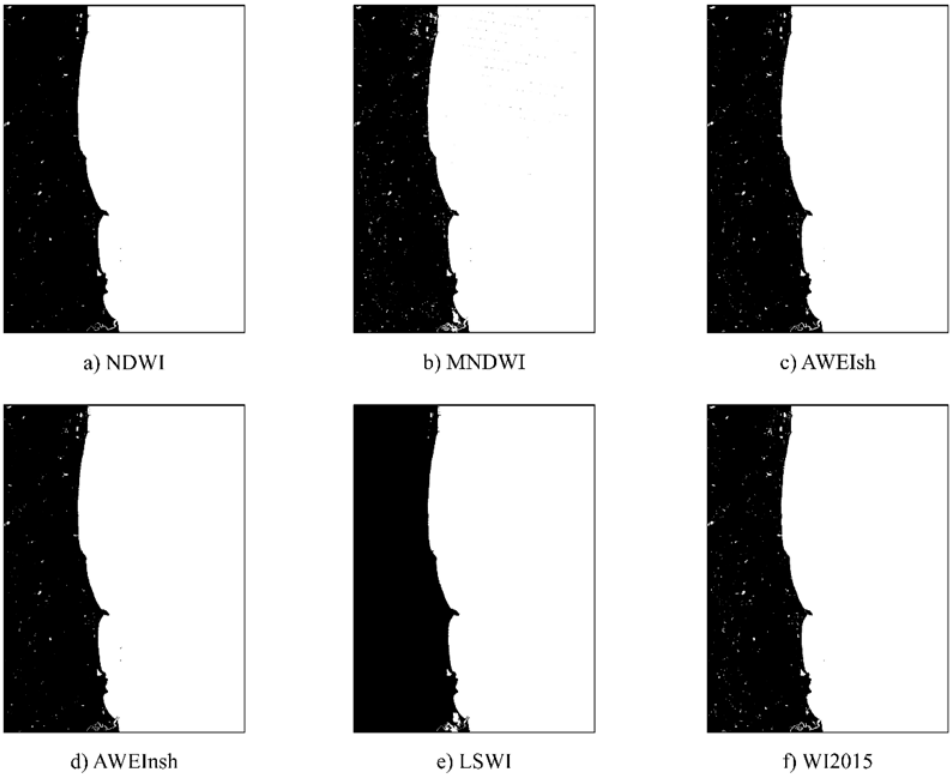

Figure 3 Water Indices Images Classify Pixels into Water and non-water Classes

Figure 3 illustrates the effectiveness of each spectral water index in separating water and land using classified maps generated from NDWI, MNDWI, AWEIsh, AWEInsh, LSWI, and WI2015 applied to the 2012 Landsat imagery. Pixels were categorized into water (white) and non-water (black) classes using threshold-based classification methods.

These classifications were performed within the Google Earth Engine (GEE) environment using the geemap Python API on Google Colab, enabling efficient processing of multi-temporal satellite imagery. The platform facilitated pre-processing steps such as cloud masking, reflectance correction, and index calculation. This allowed for automated classification and rapid visualization of shoreline positions over time.

Accuracy assessments revealed substantial differences among the six water indices. Water Index 2015 (WI2015) showed the highest shoreline extraction accuracy, achieving a Root Mean Square Error (RMSE) of 7.16 meters and the lowest Mean Absolute Error (MAE) among all indices. This performance is attributed to its use of multiple spectral bands, including SWIR, which effectively suppresses background noise from vegetation and built-up areas, as shown in Table 2.

Table 2 Accuracy Assessment of Water Indices

Water Index	Root Mean Square Error (RMSE)	Mean Absolute Error (MAE)
NDWI	23.288	16.497
MNDWI	9.374	14.707
AWEInsh	27.924	23.402
AWEIsh	15.859	13.467
LSWI	26.698	35.699
WI2015	7.156	14.010

Following accuracy validation, WI2015 was selected for multi-temporal shoreline analysis across five image years (2012, 2015, 2018, 2021, and 2024). Using the Digital Shoreline Analysis System (DSAS), a total of 380 transects were created perpendicular to the 2012 baseline at 100-meter intervals. The metrics calculated included End Point Rate (EPR), Net Shoreline Movement (NSM), and Shoreline Change Envelope (SCE) for each transect. The EPR values indicated both erosion and accretion trends along the coastline. Zone A (north) and Zone E (south) showed positive EPR values (0.753 and 0.114 m/year respectively), indicating accretion, while Zone B (central Hua Hin) exhibited the highest erosion, with an EPR of –0.821 m/year, followed by Zone C at –0.413 m/year. Zone D remained relatively stable with minor shoreline fluctuations, as summarized in Table 3 and spatially illustrated in Figure 4.

Table 3 Summary Table of EPR, SCE, NSM by Zone

Zone	EPR (m/year)			SCE (m)			NSM (m)		
	Min	Max	Mean	Min	Max	Mean	Min	Max	Mean
Zone A	-4.880	6.270	0.753	3.660	75.290	28.806	-58.600	75.290	9.036
Zone B	-7.030	2.680	-0.821	0.470	112.850	22.819	-84.380	32.170	-9.848
Zone C	-6.190	4.450	-0.413	6.880	109.190	34.031	-74.270	53.440	-4.954
Zone D	-2.720	4.080	0.201	1.530	60.940	28.404	-32.690	48.930	2.422
Zone E	-6.980	9.800	0.114	2.160	150.080	28.512	-83.700	117.580	1.361

Figure 4 The Classification of Shoreline Change Based on NSM

Based on the computed Net Shoreline Movement (NSM), the shoreline changes observed along the Hua Hin coastline are categorized into three distinct classes. These categories provide a framework for prioritizing hydrographic re-survey efforts and identifying areas of concern for coastal zone management and nautical chart updates:

5.1 Stable (NSM within ±10 meters): These shoreline segments show minimal change over 12 years, remaining within the expected uncertainty of medium-resolution satellite imagery. They indicate high shoreline stability, with negligible erosion or accretion, and pose low navigational risk. While no immediate chart updates are needed, continued monitoring is advised. As shown in the figure, these stable areas are represented in green.

5.2 Moderate Change (NSM between ±10 and ±50 meters): This range reflects noticeable shoreline movement due to gradual erosion, sediment deposition, or minor anthropogenic influences. Although not immediately hazardous, such changes may affect coastal features over time and warrant closer monitoring. Hydrographic agencies may consider medium-term verification surveys in these zones. These moderately changing areas are indicated in yellow in the figure.

5.3 Significant Change (NSM greater than ±50 meters): These transects exhibit major shoreline shifts, often driven by severe erosion, rapid accretion, storm events, or large-scale coastal development. Such extensive changes can compromise chart accuracy and create navigational hazards, especially in shallow or previously charted zones. Immediate resurvey and coastal management intervention are recommended. In the figure, these high-change areas are highlighted in red.

NSM values ranged from significant erosion and accretion, with 22 transects (approximately 6% of total) exceeding ±50 meters of change over the 12-year period. These highly dynamic areas are likely influenced by both anthropogenic factors such as seawall construction, urban expansion, and coastal tourism, as well as natural processes including sediment transport, wave action, and sea level rise. The spatial distribution of shoreline changes is classified and displayed in Figure 5.

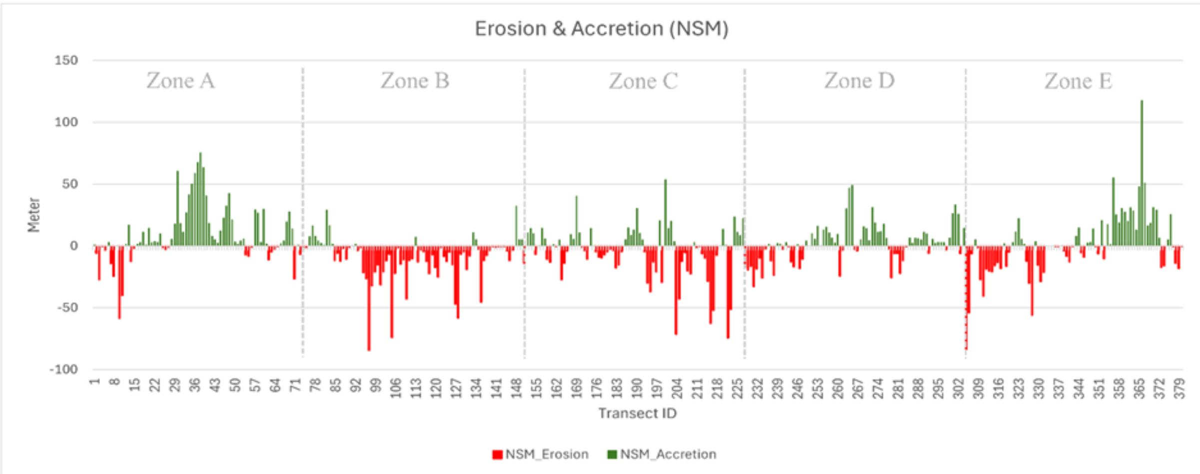

Figure 5 Graph of Erosion & Accretion by NSM Value

To provide a more nuanced understanding of temporal shoreline dynamics, Weighted Linear Regression (WLR) was applied. The WLR results revealed zones with accelerating erosion, particularly in urbanized regions, and progressive accretion in less developed areas. This temporal dimension of shoreline behavior is clearly depicted in Figure 6, which presents WLR trends along representative transects from each zone.

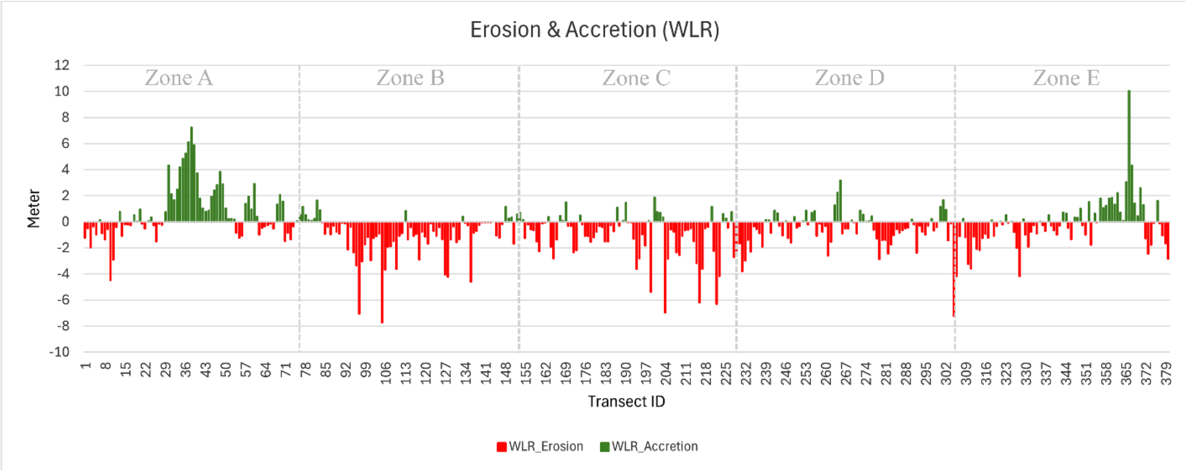

Figure 6 Graph of WLR Trends for Representative Transects

Overall, the integration of WI2015 and DSAS provides an effective methodology for capturing both spatial and temporal shoreline change patterns. The outputs from this section serve as a critical input for determining which areas require hydrographic resurvey and for prioritizing resource allocation in future coastal management plans.

6. Conclusions and Suggestions

This study investigated the effectiveness of satellite-derived water indices and geospatial techniques for shoreline extraction and change detection along Hua Hin Beach, Thailand, from 2012 to 2024. The findings highlight the potential of remote sensing to support hydrographic surveying and nautical chart maintenance in coastal areas experiencing dynamic shoreline processes. Among the six spectral water indices tested, Water Index 2015 (WI2015) demonstrated the highest accuracy, achieving a Root Mean Square Error (RMSE) of 7.16 meters. Its performance was notably superior to traditional indices such as NDWI and MNDWI, due to its multi-band formulation that enhances water–land boundary delineation, even in complex urban or vegetated environments.

The application of the Digital Shoreline Analysis System (DSAS) to WI2015-extracted shorelines enabled a detailed assessment of spatial and temporal shoreline changes using key metrics including Net Shoreline Movement (NSM), End Point Rate (EPR), and Weighted Linear Regression (WLR). The results revealed clear spatial variability throughout the study area. Zones B and C, particularly within the central urbanized stretch of the coast, exhibited consistent erosion trends, with several transects experiencing shoreline retreat greater than 50 meters. In contrast, Zones A and E showed accretion, while Zone D remained relatively stable. These patterns are influenced by both natural coastal dynamics and human activities such as infrastructure development and shoreline modification.

From a hydrographic and navigational perspective, the classification of shoreline change based on NSM values provides actionable insights for charting agencies. A total of 22 transects exceeded the ±50meter threshold, indicating areas of significant change that no longer conform to the shoreline boundaries depicted in the 2012 Thai nautical chart NC246. These transects should be prioritized for resurvey in accordance with the International Hydrographic Organization (IHO) S-44 standards to ensure accurate chart representation and navigational safety.

It is recommended that future shoreline studies in Thailand and similar coastal environments incorporate WI2015 and DSAS as a standard methodological framework. While this study offers a reliable, scalable, and cost-effective workflow, the integration of additional data, such as tidal corrections, high-resolution imagery, and field-verified ground control points, can further enhance shoreline position accuracy. Continued monitoring is essential to support adaptive coastal management, particularly in regions where tourism, infrastructure, and climate-related sea level rise are likely to intensify shoreline dynamics. The approach demonstrated in this study provides a practical contribution to the modernization of hydrographic practices in support of sustainable coastal development.

References

[1] Gens R. Remote sensing of coastlines: detection, extraction and monitoring. Int J Remote Sens [Internet]. 2010;31(7):1819-36. Available from: https://doi.org/10.1080/01431160902926673

[2] Liu X, Ma Y, Li G, Zhao Y. Coastline Evolution of the Yangtze Estuary upon Satellite Remote Sensing Analysis. Mar Geol Quat Geol [Internet]. 2014 Mar;33(2):17-24. Available from: https://doi.org/10.3724/SP.J.1140.2013.02017

[3] Nicholls RJ, Cazenave A. Sea-Level Rise and Its Impact on Coastal Zones. Science [Internet]. 2010;328:1517-20. Available from: https://doi.org/10.1126/science.1185782

[4] Mentaschi L, Vousdoukas MI, Pekel JF, Voukouvalas E, Feyen L. Global long-term observations of coastal erosion and accretion. Sci Rep. 2018;8(1):1-11

[5] International Hydrographic Organization. S-44 Edition 6.1.0, Standards for Hydrographic Surveys [Internet]. Edition 6.1.0. Principauté de Monaco: International Hydrographic Organization; 2022 Sep. Available from: https://iho.int/uploads/user/pubs/standards/s-44/S-44_Edition_6.1.0.pdf

[6] Gorelick N, Hancher M, Dixon M, Ilyushchenko S, Thau D, Moore R. Google Earth Engine: Planetary-scale geospatial analysis for everyone. Remote Sens Environ [Internet]. 2017 Dec 1;202:18-27. Available from: https://doi.org/10.1016/j.rse.2017.06.031

[7] Xu H. Modification of Normalized Difference Water Index (NDWI) to Enhance Open Water Features in Remotely Sensed Imagery. Int J Remote Sens [Internet]. 2006 Jul;27(14):3025-33. Available from: https://doi.org/10.1080/01431160600589179

[8] McFeeters SK. The Use of the Normalized Difference Water Index (NDWI) in the Delineation of Open Water Features. Int J Remote Sens [Internet]. 1996;17:1425-32. Available from: https://doi.org/10.1080/01431169608948714

[9] Xu H. Modification of Normalized Difference Water Index (NDWI) to Enhance Open Water Features in Remotely Sensed Imagery. Int J Remote Sens [Internet]. 2006 Jul;27(14):3025-33. Available from: https://doi.org/10.1080/01431160600589179

[10] Feyisa GL, Meilby H, Fensholt R, Proud S. Automated Water Extraction Index: A New Technique for Surface Water Mapping Using Landsat Imagery. Remote Sens Environ [Internet]. 2014 Jan;140:23-35. Available from: https://doi.org/10.1016/j.rse.2013.08.029

[11] Fisher A, Flood N, Danaher T. Comparing Landsat Water Index Methods for Automated Water Classification in Eastern Australia. Remote Sens Environ [Internet]. 2016 Mar;175:167-82. Available from: https://doi.org/10.1016/j.rse.2015.12.055

[12] Bishop-Taylor R, Sagar S, Lymburner L, Alam I. Sub-Pixel Waterline Extraction: Characterising Accuracy and Sensitivity to Indices and Spectra. Remote Sens [Internet]. 2019 Dec;11(24):2984. Available from: https://doi.org/10.3390/rs11242984

[13] Himmelstoss EA, Henderson RE, Kratzmann MG, Farris AS. Digital Shoreline Analysis System (DSAS) version 5.0 user guide. U.S. Geological Survey Open-File Report 2018–1179 [Internet]. Reston, VA: U.S. Geological Survey; 2018. Available from: https://doi.org/10.3133/ofr20181179

[14] Song Y, Shen Y, Xie R, Li J. A DSAS-based study of central shoreline change in Jiangsu over 45 years. Anthropocene Coasts [Internet]. 2021 Sep;4(1):115-28. Available from: https://doi.org/10.1139/anc-2020-0001

[15] Isha IB, Adib MRM. Application of Geospatial Information System (GIS) using Digital Shoreline Analysis System (DSAS) in Determining Shoreline Changes. IOP Conf Ser Earth Environ Sci [Internet]. 2020;616:012029. Available from: https://doi.org/10.1088/1755-1315/616/1/012029

[16] Chénier R, Faucher M-A, Ahola R. Satellite-Derived Bathymetry for Improving Canadian Hydrographic Service Charts. ISPRS Int J Geo-Inf [Internet]. 2018;7(8):306. Available from: https://doi.org/10.3390/ijgi7080306

[17] Scaramuzza P, Micijevic E, Chander G. *SLC Gap-Filled Products Phase One Methodology* [Internet]. Landsat Missions; 2019 Aug 2 [cited 2025 Mar 6]. Available from: https://d9-wret.s3.us-west-2.amazonaws.com/assets/palladium/production/s3fs-public/atoms/files/SLC_Gap_Fill_Methodology.pdf.

[18] Xiao X, Hollinger D, Aber J, Goltz M, Davidson E, Zhang Q. *Satellite-based modeling of gross primary production in an evergreen needleleaf forest*. Remote Sens Environ [Internet]. 2004 [cited 2025 Mar 6];89:519-34. Available from: https://doi.org/10.1016/j.rse.2003.11.008

[19] Hydrographic Department of Royal Thai Navy, Thailand. 1:40000 Nautical Chart Number 246 Hua Hin [chart]. Hydrographic Department of Royal Thai Navy; 2012.